Received: 20 January 2020 | Accepted: 21 April 2020

DOI: 10.1002/vzj2.20035

Vadose Zone Journal

SPECIAL SECTION

Transdisciplinary Contributions and Opportunities in Soil Physical Hydrology

Soil water and fuel permeability of a Cambisol in southern Brazil and its spatial behavior: A case study

Letícia Gonçalves-Maduro[1] | **Robson André Armindo**[2] | **Maria Eliza Turek**[1] | **Ole Wendroth**[3]

[1]Federal Univ. of Paraná, CEP 80035-050, Curitiba, Paraná, Brazil

[2]Dep. of Physics, Federal Univ. of Lavras, Campus UFLA, CEP 37200-000, Lavras, Minas Gerais, Brazil

[3]Dep. of Plant and Soil Sciences, Univ. of Kentucky, Ag. Sci. North N-122M, Lexington, KY 40546-0031, USA

Correspondence
Robson André Armindo, Dep. of Physics, Federal Univ. of Lavras, Campus UFLA, CEP 37200-000, Lavras, MG, Brazil.
Email: robson.armindo@ufla.br

Funding information
University of Kentucky Agricultural Experiment Station, Grant/Award Numbers: KY006093, KY006120; University of Kentucky, Grant/Award Number: 16-06-077

Abstract

The high demand for fuel derived from oil increases the risk of environmental hazard in agricultural fields caused by accidents with the operation of machines and spotting of fuel on the ground. When these accidents occur, a part of the spilled fuel infiltrates and redistributes in the soil according to the fuel's own physical properties. Most fuel products are light nonaqueous-phase liquids (NAPL) and contain compounds that are toxic and cause damage to the soil and to human health. The transport behavior of fuels in soils has been extensively studied but is lacking knowledge in specific soils with high clay content. This study aimed to evaluate the soil permeability (K) to the transport of water and fuels and their spatial variation in a Cambisol in southern Brazil. Furthermore, the question should be addressed whether K_{water} may be used to estimate K_{fuels} based on the fluid viscosities. Moreover, a spatial variance analysis should evaluate the variability between replicate repacked samples at a particular location in comparison with spatial variability caused by soil texture and bulk density differences. Results showed that K_{water} was, on average, 4.5 times smaller than $K_{gasoline}$ and 1.25 times smaller than K_{diesel}, that the correlation between measured and estimated K_{fuels} was moderately positive for the clayey soil investigated, and that a minimum set of three repacked parallel cores for each sampling location yields a local variance that is much smaller than the semivariance at any lag distance.

1 | INTRODUCTION

The release of nonaqueous-phase liquid (NAPL) substances into the soil has negative consequences for water resources and human health, as well as other living species, due to their high toxicity and mobility in the soils' vadose zone (Costa, Nunes, & Corseuil, 2009; Leharne, 2019; Machado, Carvalho, Carvalho, & Mariz, 2016). Nonaqueous-phase liquid is a generic term used to describe a class of organic liquid contaminants that are characterized by their water immiscibility, which can occur for being denser (DNAPL) or lighter (LNAPL) than water (Leharne, 2019). One of the sources for those substances are oil and its derivates, cited by the Brazilian Ministry of Environment (2015) as responsible for almost 40% of the accidents that caused environmental damage in Brazil.

Nonaqueous-phase liquids, such as gasoline and diesel, can move vertically downwards in the direction of the water

Abbreviations: LNAPL, lighter nonaqueous-phase liquid; NAPL, nonaqueous-phase liquid; OC, organic carbon.

table when they are discharged into the soil (Chevalier & Petersen, 1999). Extensive laboratory, field, and modeling studies have been carried out to evaluate many aspects of NAPL flow and transport in soils, such as the ones by Gefell, Russell, and Mahoney (2018), Hatfield and Stauffer (1993), Renshaw, Zynda, and Fountain (1997), and Zhou and Cardiff (2017). Although in many of them the chemical interactions with porous media (Kechavarzi, Soga, & Illangasekare, 2005; Kechavarzi, Soga, & Wiart, 2000; McDowell & Powers, 2003) were assessed, the transport of NAPLs is highly dependent on soil physical properties.

Some aspects of the transport of fuel in soils have been evaluated in respect to the hydraulic permeability coefficient (K_{water}) after their contamination by spills of this Newtonian substance (Gordon, Stavi, Shavit, & Rosenzweig, 2018; Takawira, Gwenzi, & Nyamugafata, 2014). In these studies, K_{water} is usually determined with soil core samples in the laboratory by applying Darcy's law (Gefell et al., 2018; Leharne, 2019), $K_{water} = q/\nabla h$, in which q is the flux density of water and ∇h is the hydraulic gradient considering a laminar flow regime. Following the same path, experiments were done with different techniques for determining K with different liquids (e.g., the soil permeability coefficient to fuels' transport [K_{fuel}]) (Leharne, 2019; van Schaik, 1969). The determination of K_{fuel} is important in many fields, such as in the analysis of soil and groundwater contamination with NAPLs from point or nonpoint sources (Comegna et al., 2019; Parnian & Ayatollahi, 2008). However, the determination of K percolating different liquids through the same sample is a difficult and time-demanding task, as identified by van Schaik (1970), who evaluated it using water and oil. In this case, substantial issues exist, such as the necessity of drying the material to remove the first liquid before the same sample could be saturated with another liquid. The complete desaturation of the material from the first percolated liquid may cause the risk of structural change besides the fact that NAPLs would influence the pore structure. To overcome this, the use of soil cores repacked with material sampled (Schäffer, Schulin, & Boivin, 2013) within a small radius of the particular location in the field would be an alternative.

In order to avoid the contamination of soils with NAPLs in experiments and those troublesome issues, K_{fuel} can alternatively be estimated by the expression $K_{fuel} = K_e g/\upsilon_{fuel}$, in which K_e is the intrinsic soil permeability, g is the gravitational acceleration, and υ_{fuel} is the kinematic viscosity of the fuel (Leharne, 2019). In this procedure, K_e is often first measured with nontoxic fluids, such as clean water or air (Hunt, Ewing, & Ghanbaria, 2014). The condition that K_e depends solely on soil and fluid properties is assumed discrediting of possible effects based on interactions between soil and fluids. Few studies have investigated K_{fuel} in agricultural fields with high clay content, in which clayey soils were used as mineral barriers to minimize downward transport and control

Core Ideas

- Can soil permeabilities (K) for water and fuels (gasoline and diesel oil) be estimated from each other?
- Repacked soil cores yield local variances smaller than spatial variances across the field.
- K_{water} and K_{fuels} show different soil spatial variability patterns.

contamination (Machado et al., 2016). Chevalier and Petersen (1999) presented a table summary of 23 papers that conducted two-dimensional NAPL experiments in the laboratory. Twenty-two of the media tested in these studies were composed of sand and one was composed of glass beads. The majority of these K_{fuel} studies reported soil texture classes other than clay (Brown & Anderson, 1983; Budhu, Giese, Campbell, & Baumgrass, 1991; Fernandez & Quigley, 1985, 1988). According to Cardoso (2011), the estimation of K_{fuel} may not be appropriate for clayey soils due to strong interactions that can occur between clay minerals and BTEX (benzene, toluene, ethylbenzene and xylene) compounds, causing changes in soil structure that would affect the soil's permeability. Fernandez and Quigley (1985, 1988) studied the influence of permeating hydrocarbons in the measurement of K_{water} for clayey soils observing increase on K_{water} in the presence of those liquids. They found K to be controlled by the viscosity and dielectric constant of hydrocarbons (nonpolar), the latter being low as compared with water (polar). Such influence was also reported by Machado et al. (2016), who indicated the electrical phenomenon that occurs around the clay particles as an important influence on the permeability. The decrease in dielectric constant is related to the reduced thickness of the double layer at the surfaces of the soil minerals and diminishes the dimensions of the porous medium (Budhu et al., 1991; Machado et al., 2016).

An important issue related to permeability coefficients, especially for toxic fluids such as NAPLs, is their spatial variability behavior. When spills occur, it is of major interest to know how the toxic fluids spread out across the landscape and what soil and other variables may underlie their spatial infiltration and percolation pattern. Strong spatial variability has been found for K percolating NAPLs (Jawitz, Annable, Demmy, & Rao, 2003; Feenstra, 2005). However, not much is known about spatial variability structure of K_{fuels}. If the spatial design of K data collection revealed structured behavior, other spatially related covariates could be found to allow coregionalization of K_{fuels} in accordance with soil texture and structure (Liang, Zhang, Wang, & Li, 2012; Wendroth, Koszinski, & Vasquez, 2011; Wendroth, Vasquez, & Matocha, 2011).

Under the hypothesis that the permeability of clayey soils to the transport of different liquids could be reliably estimated based on parallel soil samples, results of K obtained for different fluids and their spatial variability patterns in a clayey Brazilian Cambisol should be compared. Another aim was to examine whether the intrinsic permeability derived from percolation experiment water was useful to estimate permeability of the soil for fuels based on their properties (i.e., viscosity and density).

2 | MATERIAL AND METHODS

2.1 | Sampling location, soil, and fuel properties characterization

The soil material was collected at the Federal University of Paraná (UFPR), in the Applied Agricultural Sciences Farm, which is located near to Pinhais, Paraná (−25°22′38″ and 25°24′46″ S, −49°09′05″ and −49°06′40″ W). Disturbed and undisturbed soil core samples were collected in the layer between the 0- and 20-cm depth to measure sand, silt, and clay contents, dry bulk density (ρ_b), total porosity (φ), particle density (ρ_p), and saturated permeability coefficients (K). For this purpose, a regular 15-m × 15-m grid over an area of 0.5 ha was laid out resulting in 32 sampling locations. In each location, three subsamples were taken as triplicates resulting in a total of 96 samples. Another subgrid of 15 points with 25 × 25 m was designed for organic C (OC) content and macroporosity measurements, where three subsamples were taken as triplicates in the same soil layer (0–20 cm).

Air-dried soil material was sieved through a 2-mm mesh for texture and OC determination. The textural analysis was carried out based on the Bouyoucos hydrometer methodology (Gee & Or, 2002). The soil type was then established according to USDA textural triangle classification (Soil Survey Staff, 1999). Results of ρ_b were determined by the ratio between dry soil mass (105 °C for 48 h) and total soil volume, whereas the solid particle density ρ_p was measured with the pycnometer method using ethyl alcohol. Total porosity, φ, was computed as $\varphi = 1 - \rho_b/\rho_p$. The microporosity was measured draining water from soil pores with diameters larger than 50 μm using undisturbed cores on a tension table set at 60 cm of suction head. Thereby, the macroporosity was determined by the difference between φ and microporosity. The OC concentration was analyzed according to the wet combustion method (Reinheimer, Campos, Giacomini, Conceição, & Bortoluzzi, 2008).

Both gasoline and diesel oil used in this study are LNAPLs exhibiting densities smaller than that of water. The gasoline used is the common gasoline Type C commercialized in Brazil, which is colorless to yellowish, has a minimum motor octane number (MON) of 82 units, measured by the anti-knock index (AKI), a maximum of 50 mg kg^{-1} (or ppm) S content, 1% (v/v) benzene, 35% (v/v) aromatics, 25% (v/v) olefinic, and maximum vapor pressure of 69 kPa at 37.8 °C (Petrobras, 2020b). The diesel used is a diesel oil Type s50, colorless to yellowish, with 5% addition of biodiesel, maximum of 50 mg kg^{-1} (or ppm) S content, density of 820–850 kg m^{-3} at 20 °C, kinematic viscosity from 2 to 5 mm^2 s^{-1} at 40 °C, minimum derived cetane number (DCN) of 46 units, and minimum electrical conductivity of 25 pS m^{-1} (Petrobras, 2020a).

2.2 | Sample preparations to soil permeability measurement

Based on the mean value of ρ_b, obtained in situ from three undisturbed soil cores sampled in each of the 32 locations in a regular 15-m grid, nine soil cores were carefully repacked with the 2-mm sieved material according to the method described in Brazilian Association of Technical Standards (2000), Boivin, Garnier, and Tessier (2004), and Schäffer et al. (2013) for each of these 15-m grid locations. The sieved material was first oven dried at 65 °C for 48 h and then carefully filled into stainless steel cylinders of 3.35-cm height and 4.70-cm diam. The necessary mass of dry soil for each point in the field was calculated according to the local mean result of ρ_b (Brazilian Association of Technical Standards, 2000). The internal bottom of the cylinders was covered with a thin cloth to avoid loss of particles. Cores were submitted to three wetting and drying cycles in trays by capillary rise keeping the pressure head of 2 cm at the bottom of them. For each location, three groups of three cylinders underwent three saturation and drying cycles with water for consolidating the soil structure before conducting the experiments with the respective liquids. Then, they were saturated with one of the three liquids, resulting in nine cylinders for the three different liquids. This methodology aimed to represent the field conditions creating replicate samples for evaluating the three tested liquids. Thus, from the nine repacked soil cores, three were used for the transport of water, three were used for gasoline, and three were used for diesel oil. This procedure was intended to minimize local sample and field variability in order to identify the effect of the liquid being the major cause of soil permeability differences.

2.3 | Soil permeability measurement with water and fuels

The soil permeability coefficients to the transport of water (K_{water}), gasoline ($K_{gasoline}$), and diesel oil (K_{diesel}) were measured each for three of the nine repacked cores with 3.35-cm height and 4.70-cm diameter. The core samples were saturated

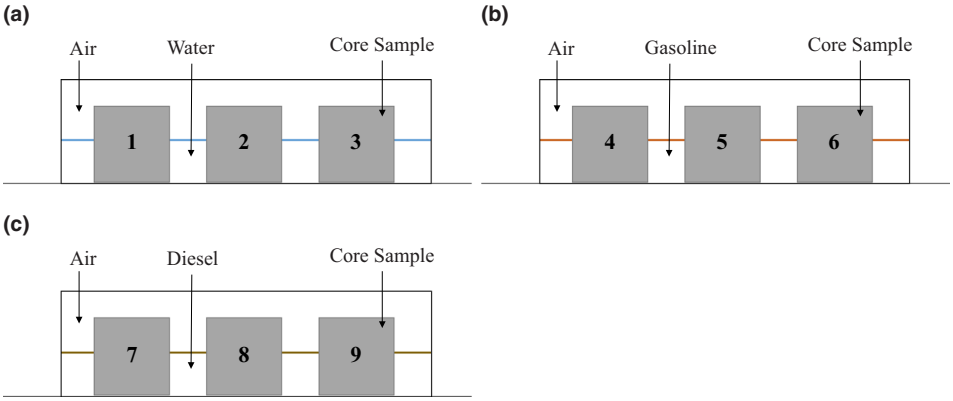

FIGURE 1 Nine repacked soil cores with the same dry bulk density, particle density, and total porosity of each point location (of the 32 assessed points) in (a) water, (b) gasoline, and (c) diesel saturation to obtain nine results of water, gasoline, and diesel permeabilities based on three measure replicates for each soil core

by capillary rise with each of the three liquids, setting the pressure boundary condition at the bottom at 2 cm (Figure 1).

Repacking a soil sample causes the structure to differ from an undisturbed sample that is taken in situ. Ideally, the same undisturbed soil cores should be used for measuring subsequently K_{water}, $K_{gasoline}$, and K_{diesel}. However, preliminary experiments showed that this procedure was not attractive because first percolating LNAPLs through the soil cores would ultimately prevent the comparison of K measured with these liquids. The reasons for this prevention are that in previous tests (a) fissures developed throughout the sample, changing its structure when measurements were done first with gasoline or diesel, and water afterwards; and (b) measuring K_{water} first complicated the percolation of fuels afterwards, because of the remaining partial water saturation of soil cores and the liquids' differing physicochemical properties (fuel density [ρ], dynamic viscosity [η], and surface tension). The NAPLs (gasoline and diesel oil) have nonpolar molecular compounds that are not dissolved in a polar solvent. These two reasons explain why measuring K_{fuels} in samples with initial water content larger than zero would have implied multiphase flow in the experimental medium and was therefore not considered in this study. Some computational approaches, such as flow simulation, multiphase computational fluid dynamics, and numerical methods would have yielded estimates that were not relevant for this study, since the main aim was to analyze measured K_{fuels} data using a simple falling-head permeameter method.

Since no way to accomplish the permeability experiments on nine parallel undisturbed soil cores collected site specifically existed (three for each liquid), the permeability measurements were carried out on three parallel repacked samples for each of the three liquids (Figure 1). This methodology was chosen because there existed no truly identical undisturbed samples with the same structure, and the effect of different liquids on permeability could therefore not have been distinguished from the effect of local variation. Instead, by repacking nine soil cores for each sampling location and obtaining 3 parallel measurements for each liquid with 3 replicates, the variation among samples was quantified.

The K_{water}, $K_{gasoline}$, and K_{diesel} were measured in analogy to Darcy's law, which was established originally for water in laminar flow regime at 20 °C for sand columns. Thereby, K_{water} and K_{fuels} were determined using the falling head method (Schramm, Warrick, & Fuller, 1986):

$$K = \frac{L}{\Delta t} \ln\left[\frac{h_{(t=0)} + L}{h_{(t=t)} + L}\right] \quad (1)$$

in which K is the saturated soil permeability coefficient (m s^{-1}) for water, gasoline, or diesel, h is the liquid pressure head (m) at $t = 0$ and at $t = t$, L is the length (m) of the soil core, and Δt is the recorded time (s) for the liquid transport through the sample.

The dynamic diesel oil viscosity (η) was measured at different temperatures using the Ford cup viscometer No. 2 apparatus (Brazilian Association of Technical Standards, 1986). Thereafter, the kinematic viscosity (υ) was determined with the ratio η/ρ (Figure 2a). Moreover, the water viscosity was calculated according to MacIntyre's (1997) equation (Figure 2b) and the gasoline viscosity according to the Brandão, Martins, and Lamego (2014) equation (Figure 2c). With K and υ data of water, the intrinsic soil permeability (K_e) results (Leharne, 2019) were calculated by

$$K_{e-water} = \frac{K\eta_{water}}{g\rho_{water}} = \frac{K_{water}\upsilon_{water}}{g} \quad (2)$$

in which $K_{e\text{-}water}$ is the intrinsic soil permeability coefficient (m^2) measured with water, η_{water}, υ_{water}, and ρ_{water} are, respectively, the dynamic viscosity (kg m^{-1} s^{-1}), kinematic viscosity (m^2 s^{-1}), and density (kg m^{-3}) of water, and g is the gravity (m s^{-2}).

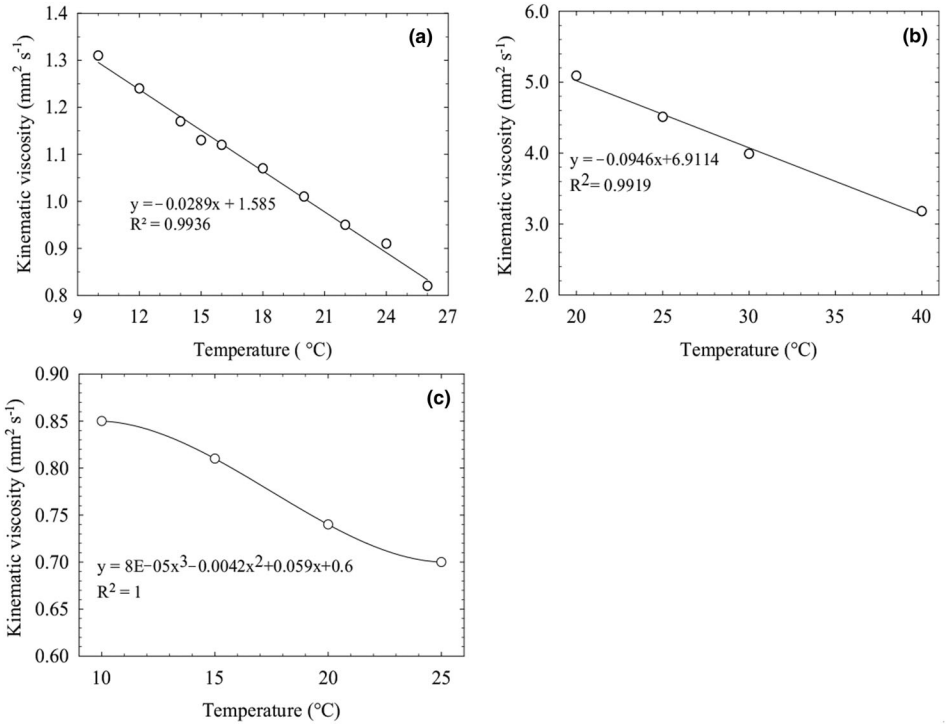

FIGURE 2 Regressions between temperature kinematic viscosity of (a) water, (b) diesel oil, and (c) gasoline

Equation 2 was also applied to find K_e measured with gasoline and diesel oil experiments. Furthermore, the permeability of each LNAPL (K_{fuel}) was estimated using an inverse relationship of Equation 2 ($K_{fuel} = K_{e\text{-}water}g/\upsilon_{fuel}$), for further comparison with measured K_{fuel} data. According to these equations, this estimation assumes that K_e measured with water and LNAPLs do not differ and that K_e depends solely on soil and fluid properties, which is discrediting of possible interaction effects between soil and these liquids. Nevertheless, a special case occurs with clays (we observed clay contents of up to 60% in our field), where K_e can also depend on the mineral interactions with the particular fluid due to its physicochemical properties and the soil-specific surface area (Cardoso, 2011; Machado et al., 2016).

The performance of estimating K_{fuel} was evaluated by using systematic and random errors with the Pearson correlation (r) and the RMSE, $\text{RMSE} = [(1/n)\Sigma(Y_{i\text{-est}} - Y_{i\text{-obs}})^2]^{1/2}$, in which $Y_{i\text{-est}}$ is the ith estimated variable, $Y_{i\text{-obs}}$ is the ith observed variable, and n is the number of analyzed values (Armindo & Wendroth, 2019; Moreno, Armindo, & Moreno, 2019).

2.4 | Spatial variability of soil permeability

Despite the fact that K_{water}, $K_{gasoline}$, and K_{diesel} could not be measured for the same soil sample, comparison of local variance among the three parallel cores used for the same given liquid, with variance between samples obtained over a spatial range of lag distances, should reveal whether results of K from the three groups of parallel cores (nine sample cores) for each location were comparable or not. The quality of comparison between mean results of K_{water}, $K_{gasoline}$, and K_{diesel} is reflected in the CV for the same liquid at the local scale. The representation of local process behavior and its dissimilarity from the behavior found for other locations is manifested in the ratio between local variance and semivariance over increasing lag distances. Many studies suggest that K data are not normally distributed, but rather log-normally distributed due to their dependence on the soil structure (Bouma, Jongerius, Boersma, Jager, & Schoonderbreek, 1977; Brejda et al., 2000; Kutílek & Nielsen, 1994; Nielsen & Wendroth, 2003; Papanicolaou et al., 2015; Warrick & Nielsen, 1980). Summary statistics and geostatistical analyses were performed using the software R and the geoR package (Ribeiro & Diggle, 2001). The soil attributes that did not follow normal distribution were analyzed using the Box–Cox (λ) transformation. According to Ribeiro and Diggle (2001), this transformation is performed applying the expression $Y^* = \log(Y)$ for $\lambda = 0$, and $Y^* = (Y^{\lambda} - 1)/\lambda$ for $\lambda \neq 0$, in which Y^* and Y are the transformed and original data, respectively. Based on the maximum log-likelihood (β), Akaike information criterion (AIC), and Bayesian information criterion (BIC), semivariogram models (Gaussian, Matérn, spherical, wave, and exponential) were fitted to the experimental semivariograms describing their nugget (C_0), sill (C), and range (a) effects (Silva, Armindo, Brito, & Schaap, 2017). These models were then applied to krige maps. Additionally,

TABLE 1 Summary statistics for the measured soil properties

Property	*N*	Max.	Min.	Mean	CV	1st qua	3rd qua	Sk	Kurt
					%				
Sand, %	32	43.8	18.8	29.82	22.5	25.0	33.7	0.29	−0.72
Silt, %	32	30.0	16.3	23.45	16.4	20.0	26.6	0.17	−1.21
Clay, %	32	60.0	31.2	46.81	16.5	41.2	53.7	−0.01	−0.99
Carbon, kg dm^{-3}	15	5.48	2.20	3.93	21.9	3.50	4.40	−0.03	−0.52
ρ_b, kg dm^{-3}	32	1.455	1.166	1.316	5.3	1.365	1.257	−0.01	0.80
φ, m^3 m^{-3}	15	0.540	0.425	0.48	6.1	0.457	0.51	0.07	−1.06
Macro, m^3 m^{-3}	15	0.18	0.09	0.12	22.7	0.100	0.13	−0.05	0.87
K_{water}, $\log_{10}$(mm h^{-1})	32	2.084	1.171	1.542	16.3	1.33	1.73	0.24	2.02
$K_{gasoline}$, $\log_{10}$(mm h^{-1})	32	2.893	1.485	2.126	16.9	1.821	2.344	0.16	2.11
K_{diesel}, $\log_{10}$(mm h^{-1})	32	2.325	0.864	1.568	24.0	1.286	1.852	−0.25	2.08
$K_{e\text{-}water}$, μm^2	32	5.70	0.689	2.06	64.1	1.01	2.77	1.14	3.55
$K_{e\text{-}gasoline}$, μm^2	32	152.9	6.95	40.13	87.5	15.3	47.10	1.56	4.96
$K_{e\text{-}diesel}$, μm^2	32	23.50	1.08	6.62	76.5	1.08	8.73	1.52	5.52

Note. φ, total porosity; Macro, macroporosity; ρ_b, bulk density; *K*, soil permeability coefficient; K_e, intrinsic permeability coefficient; carbon, organic C; 1st qua, first quartile; 3rd qua, third quartile; Sk, Skewness; Kurt, kurtosis.

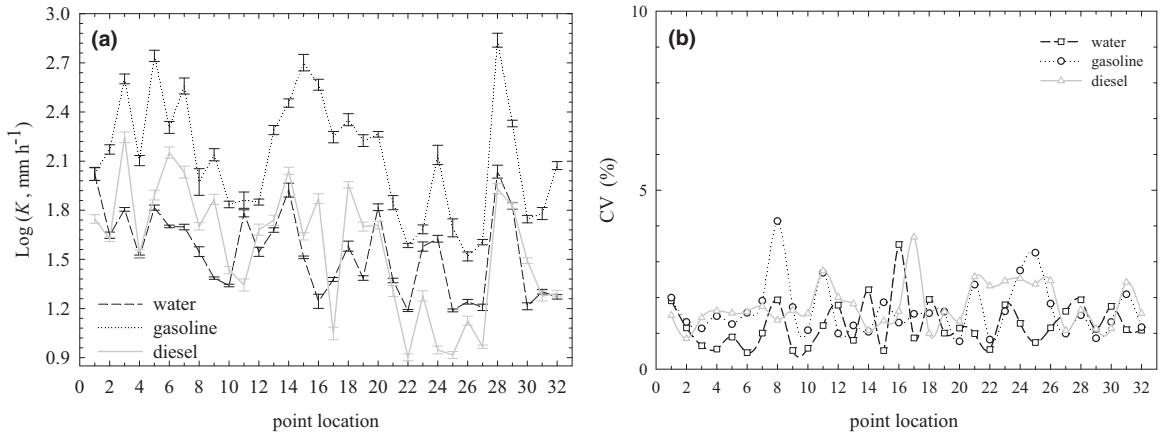

FIGURE 3 (a) Mean soil permeability coefficients (*K*) measured for water, gasoline, and diesel flows and (b) the CV of the permeability results. Results were calculated based on nine values for each liquid and field location

a matrix of Pearson correlation coefficients (*r*) represented the correlation degree between pairs of variables (Bourennane et al., 2014). The values of *r* between variables obtained at each pixel in the kriged maps were computed based on 7,531 pixels, with each pixel representing an area of 0.66 m^2.

3 | RESULTS AND DISCUSSION

3.1 | Soil properties and permeability to liquids' flux

The summary statistics obtained for physical and chemical properties of the soil, as well as permeability coefficients for the transport of water and fuels, are presented in Table 1. Based on the contents of sand, clay, and silt, the texture of the Cambisol investigated was classified as clayey (Soil Survey Staff, 1999). According to the classification presented by Warrick and Nielsen (1980), the CVs were low for φ and ρ_b and medium for the other studied properties, as found by Wang and Shao (2013) and Papanicolaou et al. (2015).

The mean results of the nine values of K_{water}, $K_{gasoline}$, and K_{diesel} for each field location together with their error bars are presented as log transforms in Figure 3a. The mean $K_{gasoline}$ (186.8 mm h^{-1}) was 4.5 times higher than the mean K_{water} (41.09 mm h^{-1}). Similar results were observed by Anderson, Brown, and Thomas (1985) and Souza, Oliveira, Machado, and Sales (2012), who measured permeability of hydrocarbons in clayey soils, and by Schramm et al. (1986), who compared *K* measured for the transport of water, xylene, kerosene,

isopropyl alcohol, and ethylene glycol. Other examples can be found in Brown, Thomas, and Green (1986), who examined K for the flux of water, acetone, and xylene.

The CV values of measured K were compared with and without log transform, since the log transform tends to reduce the difference between measured values. Wang and Shao (2013) and Papanicolaou et al. (2015) reported that K measured from undisturbed field samples and described by normal distribution can reveal CVs larger than 100%. The authors addressed different K results at the same location to the structural and textural soil heterogeneity that caused large scatter of measured K data and values of CV. Hence, this result shows that the methodology applied provided reproducible K results with the same liquid, since CV values were smaller than 5% (Figure 3b), minimizing the effect of local inherent spatial variability. When a variable presents an asymmetric normal distribution, the mean value is not a reliable representation of the data distribution and, therefore, the analysis can be biased.

The higher values of $K_{gasoline}$ might be caused by the microcracks as a result of the interaction between clay minerals and gasoline, leading to the development of preferential flow paths (Anderson et al., 1985). When hydrocarbons percolate through clayey soils, an increase in K_{water} has been observed (Fernandez & Quigley, 1985, 1988). These microcracks were visually identified in the laboratory with smaller effect in samples saturated with diesel oil. Microcracks were not identified in the sample cores saturated with water. The permeability measured for any given soil varied inversely with the liquid's dielectric constant (ε) (Schramm et al., 1986). The larger the ε value, the greater the probability of clay adsorbing the liquid, changing the attractive and repulsive forces of some minerals. The ε value is about 80.0 for water, 9.1 for gasoline, and 2.1 for diesel oil (Cardoso, 2011), indicating that the interaction of these liquids with clay minerals can cause changes within the soil cores (Budhu et al., 1991; Machado et al., 2016). As a result, due to their small ε values, both gasoline and diesel would percolate faster than water, resulting in K_{fuels} larger than K_{water}.

The mean K_{diesel} (51.1 mm h^{-1}) was 25% higher than the mean K_{water} because of the same phenomena as that occurring in case of gasoline, though less intense. Although microcracks were formed, K_{diesel} was not as enhanced as $K_{gasoline}$ due to the higher viscosity of diesel. Assuming that oil or gasoline can cause the formation of microcracks and preferential flow paths, this study corroborates the findings of Gordon et al. (2018) and Takawira et al. (2014), who reported larger measured values of K_{water} after oil spills over the soil surface. According to Gordon et al. (2018), an oil spill can trigger changes in soil structure, which enhances the increase of soil permeability. The magnitude of all K results indicates that in the case of accidental fuel spills on the soil surface and considering a single-fluid condition, the gasoline could arrive at the groundwater faster, relative to water or diesel, manifesting the necessity of immediate control measures to mitigate the consequences of such a mishap.

3.2 | Errors in the estimation of $K_{gasoline}$ and K_{diesel}

Estimates of saturated $K_{gasoline}$ and K_{diesel} were accomplished with υ of gasoline and diesel, $K_{e\text{-}water}$, and g values. However, this procedure was not a reliable way for estimating $K_{gasoline}$ (Figure 4a) and K_{diesel} (Figure 4b), as results for r and RMSE revealed for this soil. The graphs in Figure 4 visualize that the estimation of $K_{gasoline}$ underestimated the majority of the measured data (from 30 to 782 mm h^{-1}), whereas all permeability data (from 7 to 211 mm h^{-1}) measured with the transport of diesel oil were underestimated.

The results of $K_{gasoline}$ and K_{diesel} suggest that both of them should indeed be measured and not estimated regardless of the soil, since the interaction between minerals and fuels is

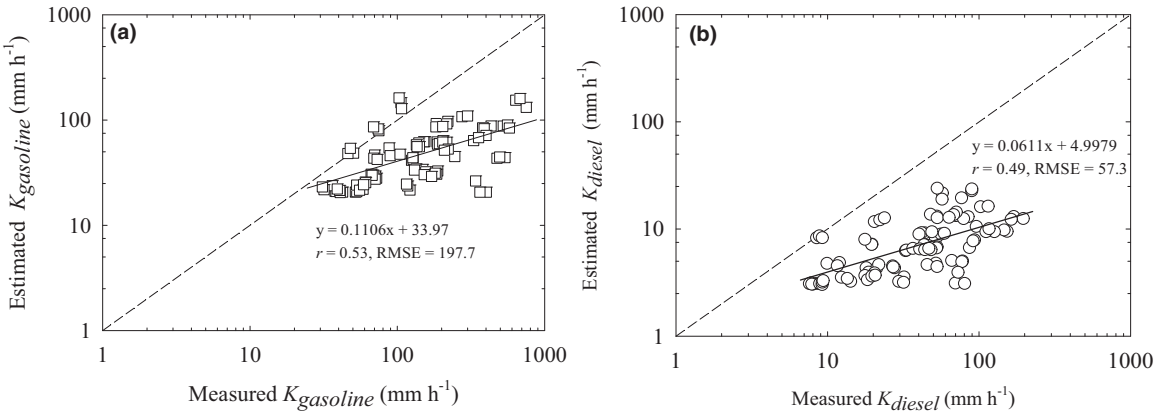

FIGURE 4 Linear correlation between the estimated soil permeabilities for (a) gasoline ($K_{gasoline}$) and (b) diesel (K_{diesel}) using the soil permeability of water (K_{water}), fuel viscosities, and gravity vs. the 32 mean measured data using these fuels

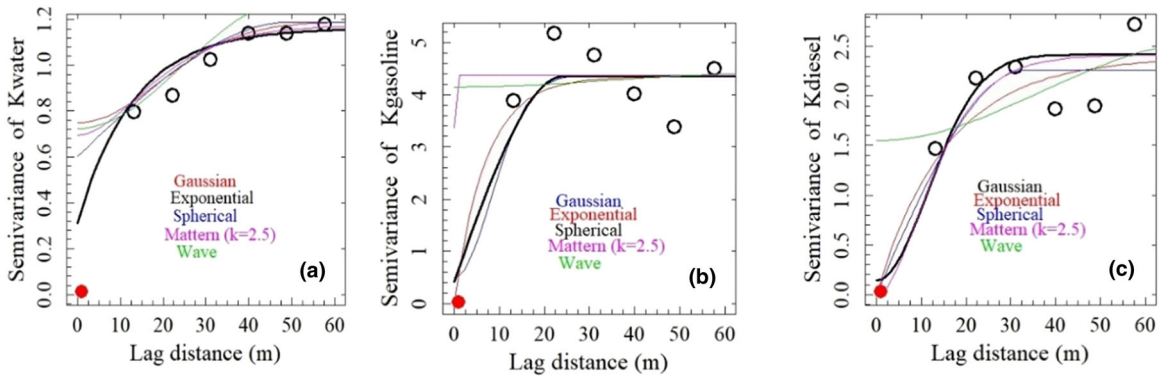

FIGURE 5 Semivariograms for *K* results and their fitted models showing that the mean variance (red bullets) resulting from the replicate repacked sample cores was much smaller than their corresponding nugget variance result and experimental semivariances obtained for lag distances between 10 and 60 m (black empty bullet). The bolder lines represent the best fitted semivariogram models for each liquid permeability. (a) water, (b) gasoline, and (c) diesel

not manifested by any variable in Equations 1 and 2, leading to discrepancies between these measured and estimated saturated permeability coefficients because gasoline and diesel had a direct impact on the pore geometry of the Cambisol as opposed to water.

The results of K_e measured in the laboratory using water, LNAPLs, and their viscosities also differed, corroborating the results Cardoso (2011) and Souza et al. (2012). These authors reported distinct results of K_e for other clayey soils using different fluids, and the addressed the relationship between ε and the soil charges (i.e., the fluid electron affinity and particle charges alter soil properties). Hunt et al. (2014) described that *K* may only be estimated for any fluid from K_e and viscosity when it is ensured that these different fluids similarly wet the same contact surface and the percolating fluid volumes are the same. Apparently, these conditions were not fulfilled in this study.

The discrepancy described between measured and estimated permeability is accented on clay minerals that have high specific surface with a large electrostatic charge—these properties induce clay minerals to adsorb water (Sendner, Horinek, Bocquet, & Netz, 2009). According to those authors, a fluid that wets the solid surface has a condition of no-slip, due to dissolved cations that interact with negative charges on the mineral surface, yielding a viscous drag close to the surface. Otherwise, a nonwetting liquid, which slides on the surface of the mineral, leads to velocity gradients in these regions. Since the fluid slip effect on the clay surface was observed at micro- or nanoscales, we cannot state for sure how relevant it is at the macroscopic level of the percolation experiments conducted in this study. A more obvious reason for the permeability behavior of the three liquids investigated is the creation of microcracks by gasoline and diesel due to their smaller values of ε, which are of a size and geometry substantial enough to strongly affect permeability through this soil structural change.

3.3 | Spatial variability of soil properties and permeability

In order to validate the assumption that the variance among parallel soil samples used in the permeability experiments is smaller than the variance between nearest sampling locations in the field, the variance for each set of three replicate repacked sample cores was applied. These variances averaged over all sampling locations were 0.0137, 0.0310, and 0.0253 $mm^2\ h^{-2}$ for K_{water}, $K_{gasoline}$, and K_{diesel}, respectively, and are plotted (red bullets) together with the semivariograms in Figure 5, where the observed local variances were much smaller than the nugget effect C_0 and the experimental variances at short lag distances.

The black bold lines in this figure denote the best fitted semivariogram models for K_{water} (exponential), $K_{gasoline}$ (spherical), and K_{diesel} (Gaussian). The fitted parameters C_0, *C*, and *a* of the best models for *K* and K_e obtained for the different liquids, sand, clay, silt, OC, ρ_b, φ, and macroporosity are shown in Table 2, together with the results of λ and the measures of the goodness-of-fit of the fitted models β, AIC, and BIC. The results justify the approach of comparing the three different sets of three samples for each specific liquid. In practical terms, the small local variance shows that nine parallel samples, from the same location, are more similar to each other than to any other sample repacked with soil material from any other location at any other distance away from any location. Thus, this approach supports the comparison between different liquids, whereas the spatial aspect was considered through the effect of soil textural differences among different locations.

All estimated ranges (*a*) were longer than the minimum sampling distance, indicating structured spatial variation and confirming that the sampling distance was chosen appropriately for the scale considered in this study. The Box–Cox transformation for *K* and K_e data was well supported in terms

TABLE 2 Fitted parameters of the best semivariogram models of chemical, physical, and soil hydraulic properties

Variable	Model	C_0	C	$C_0/(C_0 + C)$	a	β	AIC	λ	BIC
					m				
ρ_b, kg dm^{-3}	Wave	0.0030	0.0016	0.6522	45.5	43.61	−79.22	–	−73.36
OC, kg dm^{-3}	Wave	0.4393	0.2408	0.6459	54.3	−17.51	43.0	–	45.9
Sand, %	Wave	25.17	19.98	0.5575	42.8	−102.3	212.6	–	218.4
Silt, %	Wave	9.638	4.439	0.6846	20.7	−87.0	182	–	187.9
Clay, %	Spherical	16.48	47.07	0.2593	46.4	−107.5	223.1	–	228.9
φ, m^3 m^{-3}	Gaussian	0.0001	0.0008	0.1111	23.3	70.73	−133.5	–	−127.6
Macro, m^3 m^{-3}	Spherical	0.000	0.0007	0.000	24.44	33.29	−58.6	–	−55.7
K_{water}, mm h^{-1}	Exponential	0.3106	0.8524	0.2671	39.4	−138.0	284	0.2	289.8
$K_{gasoline}$, mm h^{-1}	Spherical	0.4193	3.9430	0.0961	24.3	−194.7	397.3	0.2	403.2
K_{diesel}, mm h^{-1}	Gaussian	0.1396	2.2776	0.0577	28.1	−148.0	304.1	0.2	309.9
$K_{e\text{-}water}$, μm^2	Spherical	0.0000	0.4651	0.0000	26.9	−44.94	97.87	0.2	103.7
$K_{e\text{-}gasoline}$, μm^2	Spherical	0.7499	2.0221	0.2706	33.2	−145.7	299.4	0.2	305.3
$K_{e\text{-}diesel}$, μm^2	Gaussian	0.0899	1.1041	0.0753	28.4	−83.12	174.2	0.2	180.1

Note. φ, total porosity; ρ_b, bulk density; K, soil permeability coefficient; K_e, intrinsic permeability coefficient; OC, organic C; Macro, macroporosity; C, sill; C_0, nugget; a, range; λ, Box–Cox transformation variable; β, maximized log-likelihood; AIC, Akaike information criterion; BIC, Bayesian information criterion.

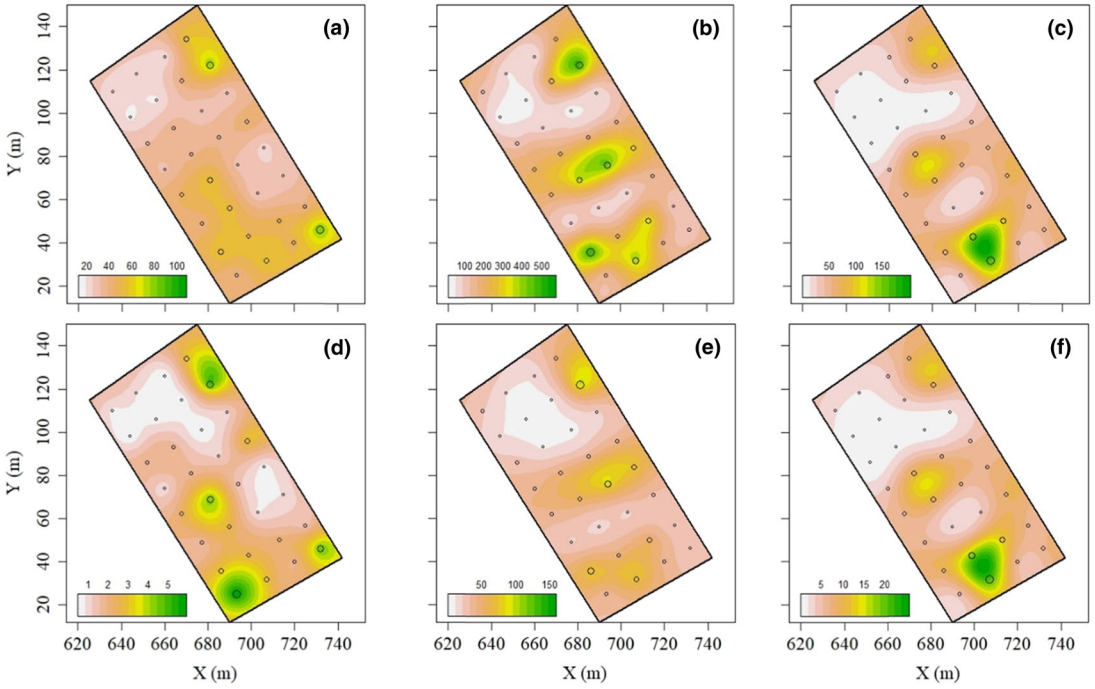

FIGURE 6 Maps of soil permeability (K, mm h^{-1}) for (a) water, (b) gasoline, and (c) diesel oil and the intrinsic permeability (μm^2) derived from measurements with (d) water, (e) gasoline, and (f) diesel oil

of the variable λ because the permeability did not reflect normal distribution behavior. The results of K were proportional to φ and macroporosity, caused by the negative correlation between K and ρ_b and between K and OC, as well as the positive correlation between K and φ and between K and macroporosity. The kriged maps for all properties assessed are presented in Figure 6. Even though resulting in different magnitudes, the maps of K for all liquids showed the similar spatial patterns, mainly in regions with relatively small values (lighter color) for $K_{gasoline}$ (Figure 6b) and K_{diesel} (Figure 6c). However, the difference in the magnitude of the results is verified. The K_e results measured with water (Figure 6d), gasoline (Figure 6e), and diesel (Figure 6f) showed regions with similar spatial pattern. Nevertheless, K_e, which should be similar regardless of the fluid used, was spatially different in this clayey soil when measured with fuels and water.

TABLE 3 Pearson correlation index (r) matrix assembled with 7,531 pixels from the soil property maps

Property	K_{water}	$K_{gasoline}$	K_{diesel}	$K_{e\text{-}water}$	$K_{e\text{-}gasoline}$	$K_{e\text{-}diesel}$
K_{water}	1	–	–	–	–	–
$K_{gasoline}$	.53	1	–	–	–	–
K_{diesel}	.59	.72	1	–	–	–
$K_{e\text{-}water}$	.81	.48	.48	1	–	–
$K_{e\text{-}gasoline}$	.51	.91	.71	.54	1	–
$K_{e\text{-}diesel}$	.59	.72	.99	.48	.71	1
Sand	−.13	−.11	−.27	.03	−.13	−.27
Silt	.17	.35	.07	.23	.41	.07
Clay	.07	.02	.25	−.11	−.04	.26
ρ_b	−.49	−.36	−.54	−.38	−.45	−.55
φ	.42	.57	.60	.28	.62	.68
Carbon	−.24	−.21	−.36	−.24	−.24	−.36
Macroporosity	−.11	−.22	−.23	−.14	−.26	−.23

Note. φ, total porosity; ρ_b, bulk density; K, soil permeability; K_e, intrinsic permeability.

The correlation between regions of ρ_b and regions of φ was manifested, as well as between OC and φ. Lastly, the inverse relation between sand and clay contents was also identified (Supplemental Figure S2). The Pearson correlation coefficients (r) obtained crossing the 7,531 pixels of each K map against the correspondent pixels of maps of the analyzed soil properties are presented in Table 3.

The correlation between K and K_e maps ranged from moderate to strong. Notwithstanding, ρ_b, φ, and macroporosity yielded medium to strong correlations and had the largest influence on the spatial results of K and K_e. Thus, K is affected by ρ_b depending more on the geometry and distribution of pores than on the texture (Pachepsky & Park, 2015).

4 | CONCLUSIONS

In this study, we measured the soil permeability coefficients (K) through transport experiments using Newtonian fluids, which were NAPL (water) and LNAPLs (gasoline and diesel), and examined their possible estimation and spatial variation in a clayey Cambisol field soil in southern Brazil. On average, $K_{gasoline}$ was 4.5 times larger than K_{water}, and K_{diesel} was 1.25 times greater than K_{water}. The estimation of $K_{gasoline}$ and K_{diesel} using the intrinsic soil permeability (K_e) measured with water was not reliable, thus suggesting that K_{fuels} should be measured for clayey soils. The variance among parallel repacked soil cores was smaller than the local variance from the same or neighboring locations at any distance. This result justified the use of the repacking approach for conducting permeability experiments with different NAPLs. Spatial range values for K_{water}, $K_{gasoline}$, and K_{diesel} varied from 24 up to 40 m. The correlations between the spatial variability maps of K_{water} and K_{fuels} were moderate, indicating that the estimation of the spatial variability maps of K_{fuels} based on K_{water} and fuel's viscosities were only of limited relevance.

CONFLICT OF INTEREST

The authors declare no conflict of interest.

ACKNOWLEDGMENTS

Coauthor (O.W.) acknowledges approval of the Director of the Kentucky Agricultural Experiment Station as Publication no. 16-06-077, and support through the SB 271 program of the University of Kentucky Agricultural Experiment Station, as well as Multistate Kentucky Agricultural Experiment Station Projects KY006093, KY006120, and W4188.

ORCID

Robson André Armindo
https://orcid.org/0000-0003-4675-8872

REFERENCES

Anderson, D. C., Brown, K. W., & Thomas, J. C. (1985). Conductivity of compacted clay soils to water and organics liquids. *Waste Management & Research*, *3*, 339–349. https://doi.org/10.1177/0734242X8500300142

Armindo, R. A., & Wendroth, O. (2019). Alternative approach to calculate soil hydraulic-energy-indices and-functions. *Geoderma*, *355*. https://doi.org/10.1016/j.geoderma.2019.113903

Boivin, P., Garnier, P., & Tessier, D. (2004). Relationship between clay content, clay type, and shrinkage properties of soil samples. *Soil Science Society of America Journal*, *68*, 1145–1153. https://doi.org/10.2136/sssaj2004.1145

Bouma, J., Jongerius, A., Boersma, O., Jager, A., & Schoonderbreek, D. (1977). The function of different types macro pores during saturated flow through four swelling soil horizons. *Soil Science Society of America Journal*, *41*, 945–950. https://doi.org/10.2136/sssaj1977.03615995004100050028x

Bourennane, H., Blanes, S. S., Conturier, A., Chartin, C., Pasquier, C., Hinschbeger, F., … Dourossin, J. (2014). Geoestatistical approach for identifying scale-specific correlations between soil thickness and topographic attributes. *Geomorphology*, *220*, 58–67. https://doi.org/10.1016/j.geomorph.2014.05.026

Brandão, A. P., Martins, R. J., & Lamego, L. S. R. (2014). Viscosity modeling for substitute mixtures for gasoline. In *Proceedings of 54° Congresso Brasileiro de Química* (pp. 97–108), Natal, Rio Grande do Norte, Brazil: Federal University of Rio Grande do Norte.

Brazilian Association of Technical Standards. (1986). *NBR 5849: Viscosity determination by Ford cup* (ABNT-NBR 5849). Rio de Janeiro: Brazilian Association of Technical Standards.

Brazilian Association of Technical Standards. (2000). *Determination of the hydraulic permeability coefficient of clay soils using falling head permeameter* (ABNT-NBR 14545). Rio de Janeiro: Brazilian Association of Technical Standards.

Brazilian Ministry of Environment. (2015). *Environmental accidents report 2014*. (In Portuguese.) Brazilian Ministry of Environment. Retrieved from https://www.ibama.gov.br/phocadownload/relatorios/acidentes_ambientais/ibama-2014-relatorio_acidentes_ambientais.pdf

Brejda, J. J., Moorman, T. B., Smith, J. L., Karlen, D. L., Allan, D. L., & Dao, T. H. (2000). Distribution and variability of surface properties at a regional scale. *Soil Science Society of America Journal*, *64*, 974–982. https://doi.org/10.2136/sssaj2000.643974x

Brown, K. W., & Anderson, D. C. (1983). *Effects of organic solvents on the permeability of clay soils* (USEPA-600/2-83-016). Cincinnati, OH: USEPA.

Brown, K. W., Thomas, J. C., & Green, J. W. (1986). Field cell verification of the effects of concentrated organic solvents on the conductivity of compacted soils. *Hazardous Waste & Hazardous Materials*, *31*, 1–19. https://doi.org/10.1089/hwm.1986.3.1

Budhu, M., Giese, R. F., Jr., Campbell, G., & Baumgrass, L. (1991). The permeability of soils with organic fluids. *Canadian Geotechnical Journal*, *28*, 140–147. https://doi.org/10.1139/t91-015

Cardoso, L. S. P. (2011). *Study of immiscible pollutants transport in soil* (Doctoral dissertation, Federal University of Bahia). Retrieved from http://www.cienam.ufba.br/publicacoes/estudo-do-transporte-de-poluentes-imisciveis-em-solos

Chevalier, L. R., & Petersen, J. (1999). Literature review of 2-D laboratory experiments in NAPL flow, transport, and remediation. *Journal of Soil Contamination*, *8*, 149–167. https://doi.org/10.1080/10588339991339289

Comegna, A., Coppola, A., Dragonetti, G., & Sommella, A. (2019). A soil non-aqueous phase liquid (NAPL) flushing laboratory experiment based on measuring the dielectric properties of soil–organic mixtures via time domain reflectometry (TDR). *Hydrology and Earth System Sciences*, *23*, 3593–3602. https://doi.org/10.5194/hess-23-3593-2019

Costa, A. H. R., Nunes, C. C., & Corseuil, H. X. (2009). Bioremediation of groundwater impacted by gasoline and ethanol using nitrate. *Sanitary and Environmental Engineering*, *14*, 265–274. https://doi.org/10.1590/S1413-41522009000200014

Feenstra, S. (2005). Soil sampling in NAPL source zones: Challenges to representativeness. *Environmental Forensics*, *6*, 57–63. https://doi.org/10.1080/15275920590913921

Fernandez, F., & Quigley, R. M. (1985). Hydraulic conductivity of natural clays permeated with simple liquid hydrocarbons. *Canadian Geotechnical Journal*, *22*, 205–214. https://doi.org/10.1139/t85-028

Fernandez, F., & Quigley, R. M. (1988). Viscosity and dielectric constant controls on the hydraulic conductivity of clayey soils permeated with water-soluble organics. *Canadian Geotechnical Journal*, *25*, 582–589. https://doi.org/10.1139/t88-063

Gee, G., & Or, D. (2002). Particle-size analysis. In J. H. Dane & C. Topp (Eds.), *Methods of soil analysis: Physical methods* (2nd ed., pp. 225–289). Madison, WI: SSSA. https://doi.org/10.2136/sssabookser5.4.c12

Gefell, M. J., Russell, K., & Mahoney, M. (2018). NAPL hydraulic conductivity and velocity estimates based on laboratory test results. *Groundwater*, *56*, 690–693. https://doi.org/10.1111/gwat.12809

Gordon, G., Stavi, I., Shavit, U., & Rosenzweig, R. (2018). Oil spill effects on soil hydrophobicity and related properties in a hyperarid region. *Geoderma*, *312*, 114–120. https://doi.org/10.1016/j.geoderma.2017.10.008

Hatfield, K., & Stauffer, T. B. (1993). Transport in porous media containing residual hydrocarbon. I: Model. *Journal of Environmental Engineering*, *119*(3). https://doi.org/10.1061/(ASCE)0733-9372(1993)119:3(540)

Hunt, A., Ewing, R., & Ghanbaria, N. B. (2014). *Percolation theory for flow in porous media* (3rd ed.). Cham, Switzerland: Springer. https://doi.org/10.1007/978-3-319-03771-4

Jawitz, J. W., Annable, M. D., Demmy, G. G., & Rao, P. S. C. (2003). Estimating nonaqueous phase liquid spatial variability using partitioning tracer higher temporal moments. *Water Resources Research*, *39*, 1192–1211. https://doi.org/10.1029/2002WR001309

Kechavarzi, C., Soga, K., & Illangasekare, T. H. (2005). Two dimensional laboratory simulation of LNAPL infiltration and redistribution in the vadose zone. *Journal of Contamination Hydrology*, *76*, 211–233. https://doi.org/10.1016/j.jconhyd.2004.09.001.

Kechavarzi, C., Soga, K., & Wiart, P. (2000). Multispectral image analysis method to determine dynamic fluid saturation distribution in two dimensional three fluid phase flow laboratory experiment. *Journal of Contamination Hydrology*, *46*, 265–293. https://doi.org/10.1016/S0169-7722(00)00133-9.

Kutílek, M., & Nielsen, D. R. (1994). *Soil hydrology*. Cremlingen, Germany: Catena.

Leharne, S. (2019). Transfer phenomena and interactions of non-aqueous phase liquids in soil and groundwater. *ChemTexts*, *5*, 1–21. https://doi.org/10.1007/s40828-019-0079-2

Liang, Y., Zhang, X., Wang, J., & Li, G. (2012). Spatial variations of hydrocarbon contamination and soil properties in oil exploring fields across China. *Journal of Hazardous Materials*, *241– 242*, 371–378. https://doi.org/10.1016/j.jhazmat.2012.09.055

Machado, S. L., Carvalho, Z. S., Carvalho, M. F., & Mariz, D. F. (2016). Field permeability tests using organic liquids in compacted Brazilian soils. *Soils and Rocks*, *39*, 301–314.

MacIntyre, J. A. (1997). *Pumps and pumping installations* (2nd ed.). Rio de Janeiro, Brazil: Livros Técnicos e Científicos Editora.

McDowell, C. J., & Powers, S. E. (2003). Mechanisms Affecting the Infiltration and Distribution of Ethanol-Blended Gasoline in the Vadose Zone. *Environment Science Technology*, *37*, 1803–18010.

Moreno, R. O., Armindo, R. A., & Moreno, R. L. (2019). Development of a low-cost automated calorimeter for determining soil specific heat. *Computers and Electronics in Agriculture*, *162*, 348–356. https://doi.org/10.1016/j.compag.2019.04.015

Nielsen, D. R., & Wendroth, O. (2003). *Spatial and temporal statistics: Sampling field soils and their vegetation*. Cremlingen, Germany: Catena.

Pachepsky, Y., & Park, Y. (2015). Saturated hydraulic conductivity of US soils grouped according to textural class and bulk density. *Soil Science Society of America*, *79*, 1094–1100. https://doi.org/10.2136/sssaj2015.02.0067

Papanicolaou, A. N., Elhakeem, M., Wilson, C. G., Burras, C. L., West, L. T., Clark, B., & Oneal, B. (2015). Spatial variability of saturated hydraulic conductivity at the hillslope scale: Understanding the role of land management and erosional effect. *Geoderma*, 243–244, 58–68. https://doi.org/10.1016/j.geoderma.2014.12.010

Parnian, M. M., & Ayatollahi, S. (2008). Surfactant remediation of LNAPL contaminated soil; effects of adding alkaline and foam producing substances. *Iranian Journal of Chemical Engineering*, *2*, 34–44.

Petrobras. (2020a). *Diesel s50, technical manual*. (In Portuguese). Petrobras. Retrieved from http://www.afeevas.org.br/intranet/arquivos/noticias/Diesel%20S50%20-%20ManualTecnico%20BR.pdf

Petrobras. (2020b). *Gasoline s50, technical manual*. (In Portuguese). Petrobras. Retrieved from http://sites.petrobras.com.br/minisite/assistenciatecnica/public/downloads/manual-tecnico-gasolina-s-50-petrobras.pdf

Reinheimer, D. S., Campos, B. H. C., Giacomini, S. J., Conceição, P. C., & Bortoluzzi, E. C. (2008). Comparison of determination methods of total organic carbon in soils. *Brazilian Journal of Soil Science*, *32*, 435–440. https://doi.org/10.1590/S0100-06832008000100041

Renshaw, C. E., Zynda, G. D., & Fountain, J. C. (1997). Permeability reductions induced by sorption of surfactant. *Water Resources Research*, *33*, 371–378. https://doi.org/10.1029/96WR03299

Ribeiro, P. J., Jr., & Diggle, P. J. (2001). geoR: A package for geostatistical analysis. *R News*, *1*, 15–18.

Schäffer, B., Schulin, R., & Boivin, P. (2013). Shrinkage properties of repacked soil at different states of uniaxial compression. *Soil Science Society of America Journal*, *77*, 1930–1943. https://doi.org/10.2136/sssaj2013.01.0035

Schramm, M., Warrick, A. W., & Fuller, W. H. (1986). Permeability of soils to four organic liquids and water. *Hazardous Waste and Hazardous Materials*, *31*, 21–27. https://doi.org/10.1089/hwm.1986.3.21

Sendner, C., Horinek, D., Bocquet, L., & Netz, R. R. (2009). Interfacial water at hydrophobic and hydrophilic surfaces: Slip, viscosity, and diffusion. *Langmuir*, *25*, 10768–10781. https://doi.org/10.1021/la901314b

Silva, A. C., Armindo, R. A., Brito, A. S., & Schaap, M. G. (2017). An assessment of pedotransfer function performance for the estimation of spatial variability of key soil hydraulic properties. *Vadose Zone Journal*, *16*(9). https://doi.org/10.2136/vzj2016.12.0139

Soil Survey Staff. (1999). *Soil taxonomy: A basic system of soil classification for making and interpreting soil surveys*. (2nd ed.). Washington, DC: USDA-NRCS.

Souza, R. P., Oliveira, I. B., Machado, S. L., & Sales, E. A. (2012). Development of an instrumented channel for multiphase flow in unsaturated soils. *Soils & Rocks*, *35*, 237–249.

Takawira, A., Gwenzi, W., & Nyamugafata, P. (2014). Does hydrocarbon contamination induce water repellency and changes in hydraulic properties in inherently wettable tropical sandy soils? *Geoderma*, *235–236*, 279–289. https://doi.org/10.1016/j.geoderma.2014.07.023

van Schaik, J. C. (1969). Improved outflow barriers for permeability measurement. *Canadian Journal of Soil Science*, *49*, 261–262.

van Schaik, J. C. (1970). Soil hydraulic properties determined with water and with a hydrocarbon liquid. *Canadian Journal of Soil Science*, *50*, 79–84.

Wang, Y. Q., & Shao, M. A. (2013). Spatial variability of soil physical properties in a region of the Loess Plateau of PR China subject to wind and water erosion. *Land Degradation & Development*, *24*, 296–304. https://doi.org/10.1002/ldr.1128

Warrick, A. W., & Nielsen, D. R. (1980). Spatial variability of soil physical properties in the field. In D. Hillel (Ed.), *Applications of soil physics* (pp. 319–344). New York: Academic Press.

Wendroth, O., Koszinski, S., & Vasquez, V. (2011). Soil spatial variability. In P. M. Huang, Y. C. Li, & M. E. Sumner (Eds.), *Handbook of soil science* (2nd ed., pp. 10-11–10-25). Boca Raton, FL: CRC Press.

Wendroth, O., Vasquez, V., & Matocha, C. J. (2011). Field experimental approach to bromide leaching as affected by scale-specific rainfall characteristics. *Water Resources Research*, *47*(6). https://doi.org/10.1029/2011WR010650

Zhou, Y., & Cardiff, M. (2017). Oscillatory hydraulic testing as a strategy for NAPL source zone monitoring: Laboratory experiments. *Journal of Contaminant Hydrology*, *200*, 24–34. https://doi.org/10.1016/j.jconhyd.2017.03.005

How to cite this article: Gonçalves-Maduro L, Armindo RA, Turek ME, Wendroth O. Soil water and fuel permeability of a Cambisol in southern Brazil and its spatial behavior: A case study. *Vadose Zone J*. 2020;19:e20035. https://doi.org/10.1002/vzj2.20035